IEEE Access
Multidisciplinary | Rapid Review | Open Access Journal

Date of publication xxxx 00, 0000, date of current version Jan 18, 2021.

Digital Object Identifier 10.1109/ACCESS.2017.DOI

Extending 5G TDD Coverage with XDD: Cross Division Duplex

HYOUNGJU JI[1], (Senior Member, IEEE), YOUNSUN KIM[1], (Senior Member, IEEE), KHURRAM MUHAMMAD[2], (Senior Member, IEEE), CHANCE TARVER[2], MATTHEW TONNEMACHER[2], TAEHYOUNG KIM[1], JINYOUNG OH[1], BIN YU[3], GARY XU[2], and JUHO LEE[1], (Fellow, IEEE)

[1]Samsung Research Seoul R&D Center, Samsung Electronics, Seoul, 06765 Korea (e-mail: hyoungju.ji, younsun, th86819, jy81.oh, juho95.lee@samsung.com)
[2]Samsung Research America, Samsung Electronics, Plano, TX 75023 USA (e-mail: k.muhammad, c.tarver, matthew2.t, gary.xu@samsung.com)
[3]Samsung R&D Institute China-Beijing, Samsung Electronics, Beijing, CO 80309 China (e-mail: bin82.yu@samsung.com)

Corresponding author: Hyoungju Ji (e-mail: hyoungju.ji@samsung.com).

ABSTRACT In this paper, an advanced duplex scheme called cross-division duplex (XDD) is proposed to enhance uplink (UL) coverage in time division duplex (TDD) carriers by utilizing self-interference cancellation (SIC) capability at a base station. With XDD, it is possible to combine TDD's ability to efficiently handle asymmetric UL and downlink (DL) traffic with frequency division duplex's coverage advantage. To do so, XDD simultaneously operates UL and DL on the same TDD carrier but on different frequency resources. Such operation leads to severe interference on the received UL signal at the base station which requires two levels of SIC implementation; antenna and digital SIC. More than 50 dB of interference is removed through the antenna SIC using electromagnetic barriers between the transmitting and receiving antennas. The remaining interference is removed by the digital SIC based on estimating the non-linear channel of the circuit at the receiver baseband. It is verified by simulation and analysis that with the proposed XDD, the UL coverage can be improved by up to 2.37 times that of TDD. To check the feasibility of XDD, a Proof-of-Concept was developed where it was observed that the benefits of XDD can indeed be realized using the proposed SIC techniques.

INDEX TERMS 5G mobile communication, Duplex, Interference, Interference cancellation, Interference Suppression, OFDM

I. INTRODUCTION

RECENTLY, the first release of the fifth generation (5G) standard, called new radio (NR), was completed in the 3rd Generation Partnership Project (3GPP) [1]. NR has been designed to support new use cases having a wide range of requirements such as enhanced mobile broadband, ultra-reliable low-latency communications, and massive machine-type communications [2, 3]. Compared to 4G Long Term Evolution (LTE), NR supports operation on higher carrier frequencies up to tens of GHz, a larger bandwidth up to 400 MHz, and a larger number of mandatory receiver antennas up to 4 at the user equipment (UE) to meet higher requirements such as peak data rate up to 20 Gbps and 1 ms latency [4].

One critical issue identified during the initial deployment of NR systems was the limited coverage [5]. Due to the higher frequency bands used for 5G in order to support wider bandwidths, a larger path loss is inevitable [6]. Another factor that impacts the NR coverage is that majority of the new 5G spectrum allocations around the globe are time-division duplex (TDD) carriers located at around 3.3 - 3.8 GHz, 28 GHz, or 39 GHz which are much higher than that of 4G [7].

TDD generally has a number of advantages over frequency division duplex (FDD). The first advantage is that time resources can be flexibly assigned to uplink (UL) and downlink (DL) considering the asymmetric ratio of traffic in both directions. DL is typically assigned the majority of the time resources to handle DL heavy mobile traffic [8, 9]. Another advantage is that channel state information (CSI) can be easily acquired via channel reciprocity so the overhead associated with CSI reports can be significantly reduced especially when there is a large number of antennas [10, 11].

Although there are advantages of TDD over FDD, there are also disadvantages. The first disadvantage is the limited coverage due to the relatively small portion of time resources for UL transmission [12]. By assigning the majority of time resources to the DL, only a small portion of time resources can be allocated to the UL resulting in a smaller coverage (see Fig. 1). Note that FDD does not have this issue since

This article has been accepted for publication in a future issue of this journal, but has not been fully edited. Content may change prior to final publication. Citation information: DOI 10.1109/ACCESS.2021.3068977, IEEE Access

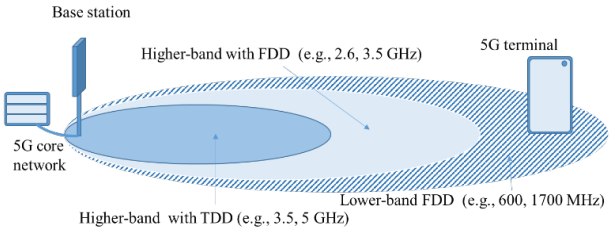

FIGURE 1. Two main aspects to coverage reduction in 5G. One is a decrease in transmission time due to the use of TDD and the other is a decrease in the propagation distance due to an increase in the center frequency.

UL has access to all time resources.[1] Another disadvantage is latency. In TDD, the timing gap between DL reception and UL transmission containing the hybrid automatic repeat request (HARQ) feedback of the corresponding DL is typically much larger than that in FDD [14, 15]. As a consequence, the HARQ round trip time in TDD is relatively longer than that of FDD, especially when the DL traffic load is high and causes a throughput loss.

There has been quite a bit of research in the wireless industry and academia [16-20] to address the shortcomings of TDD. One outcome of such research is the so-called supplementary UL (SUL) which utilizes a UL carrier in a lower frequency band in addition to a 5G carrier on a higher frequency band [16, 17]. The disadvantage of using SUL is that it incurs an additional cost in the form of an additional lower frequency carrier and implementation complexity increases at both the base station and the terminal side. Furthermore, SUL operation does not solve the fundamental problem of TDD but tries to avoid it by the use of an additional carrier. An alternative to SUL is to increase the density of 5G base stations [18, 19, 20] which would require more cell sites. From mobile network operators' (MNO) point of view, it is not attractive due to the additional economic burden. Furthermore, simple densification of 5G networks still does not address the issue of increased latency of TDD.

Another approach that could achieve coverage enhancement as well as improved latency is full-duplex (FD) [21-25]. By using FD at the base station, the UL and DL signals are received and transmitted on overlapping frequency resources [21-25]. Theoretically, spectral efficiency can be doubled and latency could be minimized. However, FD faces a number of issues in real life application. First issue is that due to using overlapping frequency resources, the received UL signal is subject to co-channel cross-link interference (CLI) [21, 23]. CLI cancellation methods include passive methods which rely on the antenna isolation between transmit and receive antennas, active methods which utilize RF or digital signal processing, and hybrid methods using a combination of these methods [43, 44, 45]. While handling co-channel CLI may require large complexity at the receiver side, it has been demonstrated by a number of researches that it is feasible. The more critical issue for FD is the handling of adjacent channel CLI. In many cellular band allocations, one operator's spectrum is located right next to the spectrum of another operator. For example, in one region of the world which now has nationwide 5G coverage, three MNOs are allocated 5G spectrum as follows.

- MNO#1: 3.42 GHz - 3.5 GHz (3GPP band n78)
- MNO#2: 3.5 GHz - 3.6 GHz (3GPP band n78)
- MNO#3: 3.6 GHz - 3.7 GHz (3GPP band n78)

Assume that MNO#2 is deploying FD in it networks. In such a case, it would have to handle not only the co-channel CLI within its own spectrum but also the adjacent CLI generated by the other two MNOs due to imperfect filtering on the DL transmission. In a conventional TDD system, such adjacent channel CLI would not be problematic since all three operators would be using the same UL-DL time resource configuration. In short, there would not be any adjacent channel CLI to begin with. Handling adjacent channel CLI is challenging due the difficulty of implementing active and passive cancellation. For active cancellation, the complexity at the receiver side would be extremely high since it requires the entire operation must be done without *a priori* knowledge of the DL transmitted signals of another MNO. Furthermore, for passive cancellation to work, the MNO who is generating the adjacent channel needs to implement interference suppression on it's own network for the benefit of the MNO who is deploying FD. In other words, for MNO#2 to deploy FD, MNO#1 and MNO#3 would need to share some of the financial burden.

This paper proposes an advanced duplex scheme, referred to as cross division duplex (XDD), and its base station implementation to overcome the coverage limitations imposed by TDD systems. XDD realizes simultaneous DL and UL operation within a TDD carrier by using different TDD configurations across different frequency regions. By doing so, XDD is able to adapt for different UEs individually with different TDD configurations. For UEs located at cell edge whose main concern is coverage, UL heavy TDD configuration is used to guarantee sufficient time resources on the UL to improve UL coverage. For UEs close to the cell center with good signal conditions, DL heavy TDD configuration is used to guarantee high DL throughput. These heterogeneous TDD configurations operate simultaneously at a base station within a single TDD carrier.

The performance of XDD is verified using numerical evaluation as well as actual hardware and software based Proof-of-Concept (PoC). It was observed that an XDD system utilizing UL time resource that is 5 times that of a conventional TDD system could extend the UL coverage area by a factor of 2. In the PoC, antenna SIC is used to minimize the leakage power from TX antenna to RX antenna. In addition, digital SIC is used to handle any residual interference after antenna SIC. It was observed that the DL out-band signal flowing into the UL receiver path can be effectively suppressed below the noise floor level to guarantee the UL receiver performance.

[1]The downside of FDD, however, is that it cannot efficiently handle asymmetric UL/DL traffic [13].

This article has been accepted for publication in a future issue of this journal, but has not been fully edited. Content may change prior to final publication. Citation information: DOI 10.1109/ACCESS.2021.3068977, IEEE Access

Also, by combining digital pre-distortion (DPD) [37] at transmitter (TX) path and digital SIC at receiver (RX) path, the out-band interference from the DL signal to the UL can be effectively mitigated such that the guardband between the UL and DL signal can minimized. The key contribution of this paper are the following:

- A new duplex method, XDD, to address the coverage limitation of 5G TDD carriers. With XDD, the base station can improve the uplink performance at cell boundary regions and while being able to simultaneously handle DL heavy asymmetric traffic.
- A passive SIC method using multiple choke walls that is precisely designed to isolate co-channel CLI over a wideband. Unlike active SIC method where the complexity becomes prohibitive for large number of antennas, the proposed passive method is well suited even for massive MIMO [52].
- State of the art digital SIC to handle the remaining co-channel CLI. The digital SIC is designed to operate in conjuction with digital pre-distortion (DPD) and antenna isolation. The digital SIC provides a high degree of flexibility for XDD in that the UL and DL subbands can be flexibly located over the bandwidth depending on the need of the use cases.

The rest of this paper is organized as follows. The overall concept of XDD is discussed in Section II. Design principles of XDD system architecture are described in Section III. Simulation results are provided in Section IV. The feasibility and effectiveness of XDD are verified based on PoC results in Section V. Finally, conclusions are drawn in Section VI.

II. XDD CONCEPT

A. REVIEW OF DUPLEX SCHEMES

Before discussions on XDD, it should be worthwhile to briefly summarize the duplexing schemes that have been used in conventional cellular systems. In early cellular systems such as 3G, FDD was dominantly used due to the narrowband nature of wireless signals [26, 27]. Although TDD was introduced to supplement FDD in 3G, it was not popular due to limitations in coverage [28]. However, with wireless traffic expanding exponentially, scale, especially due to DL heavy traffics such as wireless internet and video, the benefits of TDD became evident [13]. In fact, for many of the 4G systems utilizing FDD, the UL is often underutilized while the DL is under heavy use. In 5G, most of the new carriers are TDD carriers and therefore to address such issues [12]. Of course, the fundamental problem of coverage limitation of TDD is still not addressed.

There have been attempts to use TDD and FDD at the same time to combine the benefits of both duplexing schemes in proposals such as hybrid division duplex [29-31]. Although the approaches in [29-31] are easy in concept, realizing an actual cellular system based on such a concept is no easy task. There are a number of challenges that need to be addressed. First, within a base station, the transmitted signal causes self interfering co-channel CLI on the received signal. Second, between base stations of the same MNO, there is CLI due to the difference in duplex direction at a given time. Third, between base stations of different MNOs, there is adjacent channel CLI due to leakage signal from the neighboring channel. The purpose of this paper is to propose a new duplexing scheme using the current NR specifications that combines the benefits of TDD and FDD but designed so that the above challenges can be addressed effectively.

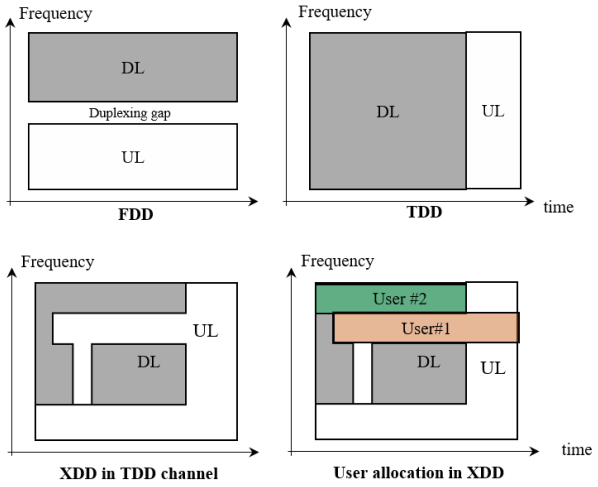

FIGURE 2. The concept of XDD and user allocation for XDD. In XDD, users are allocated UL/DL ratio depending on the user-specific scenario and QoS targets.

B. XDD: CROSS DIVISION DUPLEX

The concept of XDD is depicted in Fig. 2. XDD is a duplexing method in which duplexing can be implemented in either time domain, frequency domain, or both domains within a single TDD carrier depending on the needs of the deployment scenario. A base station can schedule non-overlapping resources (in frequency-domain) to terminals so that DL and UL transmissions occur even in the same time instance. In other words, a cell-edge terminal can be assigned to transmit continuously on UL resources (user #1 in Fig.2) while DL transmissions are being made at the base station side to serve other users (user #2 in Fig.2) at the same time. It is worth noting that the mobile station does not requires any additional implementation for XDD. As a result, the accumulated UL energy at the base station can be larger for XDD which would increase the coverage beyond what is possible for TDD. Note that since a typical cell edge terminal requires only a narrow frequency resource, the remaining portion of the carrier can be used for DL transmissions. As mentioned beforehand, such an operation requires advanced SIC capability at the base station to handle the self-interference. In addition, according to the presence of UL transmission, the base station can effectively receive the UL signal by abortively applying self-interference cancellation. One characteristic of XDD worth noting is that it requires no change on the terminal side.

This article has been accepted for publication in a future issue of this journal, but has not been fully edited. Content may change prior to final publication. Citation information: DOI 10.1109/ACCESS.2021.3068977, IEEE Access

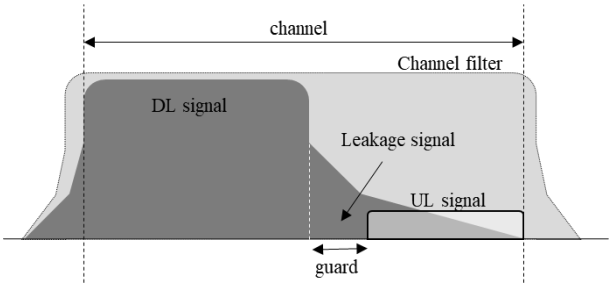

FIGURE 3. XDD self-interference scenario in the frequency domain.

Conventional TDD terminals can be supported by a XDD base station without any modification.

C. REQUIREMENTS AND CHALLENGES FOR XDD IMPLEMENTATION

To implement XDD at the base station, the following requirements should be met. First, it is necessary to prevent analog-to-digital converter (ADC) saturation [32, 33] due to the high power DL signal coupling to the UL path. When ADC saturation occurs, the received UL signal is severely degraded and cannot be restored even after digital SIC. Second, the residual interference must be reduced below the receiver's noise level before UL demodulation and decoding operation. In many cases, even a small level of interference left after SIC could make it impossible to use high order modulations such as 64QAM and 256QAM. Finally, the frequency separation between the UL and DL acting as the guard band should be minimized. If SIC is not properly implemented and there is a significant level of residual interference, the guardband between a DL signal and a UL signal would need to be increased causing a loss of resource efficiency (see Fig. 3).

There are a number of challenges in achieving the requirements described above, some of which are as follows:

1) Modeling of the non-linear self-interference channel: In order to effectively operate the SIC on the self-interference which has time varying non-linear characteristics, active components (e.g., high power amplifier, cascaded power drivers) and passive circuits (e.g., filter) must be modeled accurately [34, 35].
2) Interference oversampling and synchronization: In order to remove the interference signal, the relationship between the interference signal and the original signal must be closely observed. To this end, the receiver needs to perform oversampling at a rate of 5-7 so as to obtain perfect synchronization, which is very difficult for a system with large bandwidth.
3) Internal power coupling and crosstalk: No matter how much interference signal is reduced at the receive antenna, if the crosstalk between the components in the internal circuitry cannot be suppressed sufficiently, it deteriorates the performance of interference cancellation.
4) SIC method in the RF domain: In order to prevent ADC saturation at the receiver chain, it is necessary to suppress the signal as much as possible at the RF stage. The active cancellation method studied so far is capable of an acceptable level of cancellation, but the complexity is too high to be used for a bandwidth over 100 MHz and more than 32 multi-antennas (typical 5G base station). Therefore, a low-complexity RF SIC method that can be applied regardless of the number of antennas and bandwidth is required for commercial viability.
5) SIC method in the digital domain: Various digital SIC methods are studied in the literature. However, many state-of-the art solutions are impractical in implementations due to fixed-point processing and the high algorithmic complexity In order to actually use XDD, it is necessary to implement an algorithm that can be implemented in an FPGA to reduce residual interference.

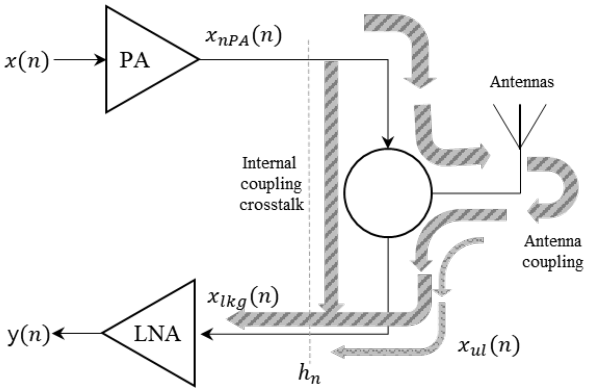

FIGURE 4. The system model for self-interference at the base station.

Based on these requirements and challenges, we propose a system architecture that maximizes the benefits of XDD in the following section.

III. DESIGN OF XDD SYSTEM ARCHITECTURE

A. SYSTEM MODEL

Figure 4 illustrates the SIC system model for typical TDD base station architecture. Let $x(n)$ be the transmit baseband signal for time sample n. The non-linear PA output signal $x_{nPA}(n)$ can be expressed using parallel Hammerstein Model [36] as follows:

$$x_{nPA}(n) = \sum_{odd\ p}^{P} \sum_{k=0}^{N-1} f_{p,k} x(n-k)|x(n-k)|^{p-1}, \quad (1)$$

$$= \sum_{odd\ p}^{P} f_{p,n} \circ x(n)|x(n)|^{p-1}, \quad (2)$$

where P is the maximum non-linearity order, $f_{p,n}$ is the PA impulse response of length $N-1$ for the nonlinear order p, and the operator $\circ$ represents the convolution operator. Expressing the coupling response from TX to RX chain (e.g.,

This article has been accepted for publication in a future issue of this journal, but has not been fully edited. Content may change prior to final publication. Citation information: DOI 10.1109/ACCESS.2021.3068977, IEEE Access

PA to Low-noise amplifier (LNA)) as h_n, the leakage signal at the RX chain $x_{lkg}(n)$ can be expressed as

$$\begin{aligned} x_{lkg}(n) &= h_n \circ x_{nPA}(n) \\ &= \sum_{odd\ p}^{P} h_{p,n} \circ x(n)|x(n)|^{p-1}, \end{aligned} \tag{3}$$

where $h_{p,n}$ is the unknown coupling response for non-linearity order p and time sample n. The received RX signal $y(n)$ can be expressed as

$$y(n) = x_{ul}(n) + x_{lkg}(n) + z(n), \tag{4}$$

where $x_{ul}(n)$ is the desired UL signal and $z(n)$ is the additive Gaussian random noise. To remove leakage signal $x_{lkg}(n)$ from the received signal $y(n)$, the base station firstly needs to reduce the leakage power level to prevent ADC saturation and then, needs to emulate leakage signal from the transmitted signal. That is,

$$\hat{x}_{lkg}(n) = \sum_{odd\ p}^{P} \sum_{\tau} \hat{h}_{p,n,\tau} x(n-\tau)|x(n-\tau)|^{p-1}, \tag{5}$$

where $\hat{h}_{p,n,\tau}$ is the estimated leakage channel coefficient for time delay τ. Two dominant components which contribute to the leakage channel are surface wave leakage and near field coupling. The receiver can handle these two components together with a combined set of leakage channel coefficients.

In the following subsection, three SIC steps are described for the XDD base station. These are adjacent channel leakage ratio (ACLR) reduction with DPD, surface wave and near field coupling cancellation with choke wells, and the digital SIC for handling residual interference at the base station.

B. SELF-INTERFERENCE CANCELLATION

Effective SIC is critical for XDD operation. We accomplish this with three different technologies that work together which we will detail in this section. Firstly, we linearize the transmit chain, reducing the ACP which falls onto the downlink band. Secondly, we improve the isolation in the antennas so that less DL interference will flow into the UL antennas. Lastly, we use Digital SIC to remove any remaining interference in the digital baseband.

1) Step 1: ACLR reduction using DPD

The TX chain includes the primary PA as well as many pre-driver stages and filters. Each of these are necessary in a commercial product and contribute to the nonlinearities and frequency shaping experienced in the leakage.This cascade of nonlinearites in the TX Chain can be effectively modeled as a single nonlinear system shown in Fig 5. An increased linearity can be achieved by applying DPD on the transmit signal after which (1) can be rewritten as

$$\tilde{x}_{nPA}(n) = \sum_{odd\ p}^{P} f_{p,n} \circ \tilde{x}(n)|\tilde{x}(n)|^{p-1}, \tag{6}$$

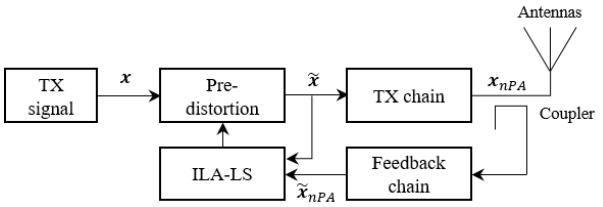

FIGURE 5. XDD SIC sub-system for Step 1 DPD

where $\tilde{x}(n)$ is the pre-distorted TX signal at the baseband.

Typically, the generalized memory polynomial (GMP) model is widely used as the pre-inverse model for the non-linearity of the systems, memory effects, and cross-memory effects [38]. The output of pre-distorted signal $\tilde{x}(n)$ can be expressed as

$$\begin{aligned} \tilde{x}(n) &= \sum_{p\in P_a} \sum_{m\in M_a} a_{p,m} x(n-m)|x(n-m)|^{p-1} \\ &+ \sum_{p\in P_b} \sum_{m\in M_b} \sum_{l\in L_b} b_{p,m,l} x(n-m)|x(n-m-l)|^{p-1} \\ &+ \sum_{p\in P_c} \sum_{m\in M_c} \sum_{l\in L_c} c_{p,m,l} x(n-m)|x(n-m+l)|^{p-1}, \end{aligned} \tag{7}$$

where $a_{p,m}$, $b_{p,m,l}$, and $c_{p,m,l}$ represent coefficients for polynomials for the pre-distortion. P_a and M_a are the index arrays for aligned signal and envelope. P_b, M_a, and L_b are the index arrays for signal and lagging envelope. P_c, M_c, and L_c are the index arrays for signal and leading envelope.

To maximize the linearity of the TX chain, the indirect learning architecture with least-squares (ILA-LS) is utilized [42]. Let $\boldsymbol{\beta}$ be a vector collecting all the GMP coefficients, e.g., $a_{p,m}$, $b_{p,m,l}$, and $c_{p,m,l}$ in (7). The key of ILA-LS is to learn the coefficients that minimize the LS errors between the output of the pre-distorted signal $\tilde{x}$ and the post-distorted signal $\hat{x}$. By letting $\tilde{\mathbf{x}} = [\tilde{x}(0)\ \tilde{x}(1)\ ...\ \tilde{x}(N-1)]^T$ and $\hat{\mathbf{x}} = [\hat{x}(0)\ \hat{x}(1)\ ...\ \hat{x}(N-1)]^T$, $\hat{\mathbf{x}}$ is given by

$$\hat{\mathbf{x}}_{nPA} = \tilde{\mathbf{X}}_{nPA} \cdot \boldsymbol{\beta}, \tag{8}$$

where $\tilde{\mathbf{X}}_{nPA}$ is a matrix representation of the GMP for $\tilde{x}_{nPA}$ where columns correspond to basis functions of the polynomial. Thus the optimum $\hat{\boldsymbol{\beta}}$ can be expressed as

$$\hat{\boldsymbol{\beta}} = \arg\min_{\boldsymbol{\beta}} \left\| \tilde{\mathbf{x}} - \tilde{\mathbf{X}}_{nPA} \cdot \boldsymbol{\beta} \right\|, \tag{9}$$

and we have

$$\hat{\boldsymbol{\beta}} = \left(\tilde{\mathbf{X}}_{nPA}^H \tilde{\mathbf{X}}_{nPA} \right)^{-1} \tilde{\mathbf{X}}_{nPA}^H \tilde{\mathbf{x}}. \tag{10}$$

To do this, the output of PA signal, $\tilde{x}_{nPA}(n)$, is captured before the antenna port and fed into a GMP estimator to compare pre and post-distorted signals. Noting that this process requires an additional RX chain that includes a coupler, attenuator, and ADC. Once $\hat{\boldsymbol{\beta}}$ is obtained, this vector is applied to pre-distortion and iteratively generates $\tilde{x}_{nPA}(n)$

This article has been accepted for publication in a future issue of this journal, but has not been fully edited. Content may change prior to final publication. Citation information: DOI 10.1109/ACCESS.2021.3068977, IEEE Access

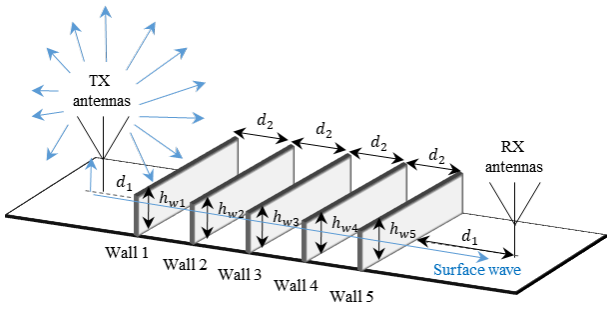

FIGURE 6. XDD SIC sub-system for Step 2.

until convergence is achieved. To end this, Tikhonov regularization is used to improve the numerical stability of the LS calculation [39]. This approach will place a small penalty on the magnitude of each element of $\boldsymbol{\beta}$ and also makes it suitable for FPGA implementation.

Using the DPD, ACLR after PA can be reduced by more than 10 dB without degrading the error vector magnitude (EVM) at the TX chain.

2) Step 2: Surface wave leakage and near field coupling cancellation with multiple choke walls

After enhancing the linearity of the TX chain, the next step is to cancel the surface wave leakage between TX and RX antennas. To do this, a novel antenna SIC is used, which relies on multiple choke walls forming a corrugated plane surface. The structure of the choke wall is illustrated in Fig. 6. Since the surface wave is composed of transverse electric (TE) and transverse magnetic (TM) waves, both types of waves can be canceled. By cascading the perfect electrical conductor (PEC) and the perfect magnetic conductor (PMC), both TE and TM waves can be suppressed [41]. There are three design parameters for choke wall: height of each wall, the distance between TX/RX antenna and the closest choke wall d_1, and inter-wall distance d_2.

There are two approaches to design the wall height, the first is to use a height between $\frac{\lambda}{4} < d < \frac{\lambda}{2}$ for achieving high attenuation using walls, and the second is to have a different height between walls to cancel the wideband signal. One example of using two choke walls is to have the height of the first and second walls as $(\lambda + \delta_1)/2$ and $(\lambda + \delta_2)/2$, respectively. The values of δ_1 and δ_2 are obtained to achieve the best suppression across the target bandwidth. Next, the distance d_1 should be considered to avoid the cancellation of the reflected wave and radiated wave at the TX antenna. To prevent 180 degrees of phase shift in the reflected wave, d_1 should be approximately $\frac{1}{4}$ of wavelength. Lastly, d_2 should be selected by considering the thickness of the wall (t). When $t \ll d_2 + t < \frac{\lambda}{2}$, there will be one non-evanescent mode presented within the corrugations. Hence, the thickness of the wall should be thin enough and the distances between two adjacent walls should be less than half of the wavelength. All the parameters are obtained from high-frequency electromagnetic solvers (HFSS) to target the design requirement of the XDD base station.

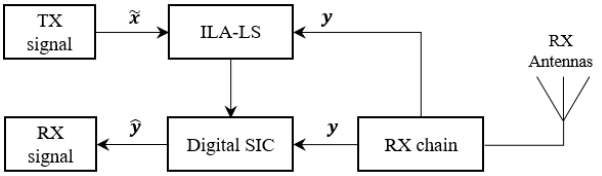

FIGURE 7. XDD SIC sub-system for Step 3.

Together with the surface wave canceling, the near-field coupling should be minimized together. In general, as the distance between the TX and RX antennas is increased, the coupling effect is decreased. In addition to coupling power reduction, the number of choke walls can be increased to reduce surface wave even more. However, considering the form factor of antenna port, the dimension of the antenna part will be more than double. From the measurements from XDD PoC, with approximately 4 times of wavelength separation between TX and RX antennas, there can be at least 5 walls. As a proper design of Walls, in total 55 dB isolation can be observed between TX and RX antenna. Isolation performance of choke wall and separation contributes 10 dB and 45 dB with the same polarization, respectively.

3) Step 3: Digital SIC for reducing residual leakage power

Once DPD and antenna SIC are utilized, the next step is to estimate the leakage channel coefficient $\hat{h}_{p,n,\tau}$ and delay τ for canceling out the remaining leakage signal from the received signal. As depicted in Fig. 7, another GMP model is used to estimate the non-linearity of the overall leakage channel. Instead of calculating a pre-inverse model of the PA in the TX, the goal of leakage channel estimation is to model the non-linear channel from the PA to RX chain. Given that the input and output signals of the PA are known, the system can be solved directly by LS in (10).

Note that, unlike FD, the received UL signal interferes with the adjacent leakage signal of the DL TX. This infers that when the ACL power level of the DL signal is suppressed below the level of noise floor by step 1 and 2, UL performance will not be degraded without applying the step 3 SIC. On the other hand, if the ACL power level is relatively higher, all interference power received at the RX path must be removed.

IV. XDD PERFORMANCE ANALYSIS

A. SIC BUDGET FOR XDD OPERATION

Table 1 shows the SIC budget calculations for an XDD system designed for a 30 dBm output power per antenna at the TX in a 100 MHz bandwidth (BW). At the TX chain, 80% of BW is used for transmission while the remaining 20% of BW is not used. At the RX chain, remaining 20% is used for UL reception. The values of X and Y are design parameters, which are antenna SIC and ACLR performance, respectively. To compare the results between the SIC budget analysis and PoC, 91 dB pathloss is set as a reference. The TX and RX

This article has been accepted for publication in a future issue of this journal, but has not been fully edited. Content may change prior to final publication. Citation information: DOI 10.1109/ACCESS.2021.3068977, IEEE Access

TABLE 1. XDD SIC Budget.

Quantity	Value	Unit
Channel bandwidth	100	MHz
TX output power (1)	30	dBm
ACLR (2)	Y	dBc
DL AC power (3)	(1) - (2)	dBm
Antenna SIC (4)	X	dB
Leakage power at RX antennae (5)	(1) - (4)	dB
ACL power at RX antenna (6)	(3) - (4)	dBm
RX bandwidth for XDD	20	MHz
UE TX power (9)	23	dBm
Cable loss (7)	10	dB
Pathloss (10)	91	dB
LNA gain (8)	20	dB
RX leakage power at ADC input (11) (w/ cable loss)	(5) - (7) + (8)	dBm
RX ACL power at ADC input (16)	(6) - (7) + (8)	dBm
RX UL received power at ADC input (12)	(9) - (10) - (7) + (8)	dBm
Noise level (inc. 3dB noise figure) (13)	-91	dBm
LNA gain (14)	20	dB
Noise level at ADC input (15)	-71=(13)+(14)	dBm
Maximum input level at the ADC (58 dB dynamic range)	-13	dBm
Remaining ACL power	(16)-(15)	dB
Digital SIC budget	(11)-(12)	dB

antennas are designed to have RF isolation of at least X dB by using dedicated antennas and isolation walls as described in Section IV. The TX chain has various nonlinear components, specifically the cascaded power drivers and the high-power PA that cause adjacent channel leakage (ACL) to out-band (unused band) where XDD UL reception will operate.

Based on the design parameters of X and Y, the necessary region for digital SIC and the required digital SIC budget can be depicted in the upper and lower sub-figure in Fig. 8, respectively. The blue region in the upper sub-figure indicates the region where the remaining residual interference is lower than the noise figure level. In this case, digital SIC is not required and the UL signal can be decoded without interference. Otherwise, the total DL leakage power interferes with the UL signal and the receiver requires digital SIC in the in-band region. For example, if 55 dB isolation is achieved with antenna SIC with 50 dBc ACLR, the required SIC at the digital level would be 43 dB. Meanwhile, when ACLR is increased to 60 dBc, digital SIC is not necessary at all.

B. UL COVERAGE ENHANCEMENT WITH XDD

To verify the coverage extension performance with XDD, link level simulation has been performed. The carrier frequency and subcarrier spacing are assumed as 3.5 GHz and 30 kHz, respectively. To consider the coverage limited environments of cell-edge terminals, the number of allocated resource blocks (RBs) and the corresponding occupied channel bandwidth was assumed as 4 RB and 1.44 MHz. Other parameters for the link simulation are shown in Table 2. For TDD UL, only one packet is transmitted while 5 repetitions are used for XDD UL. For repetitive transmission of XDD,

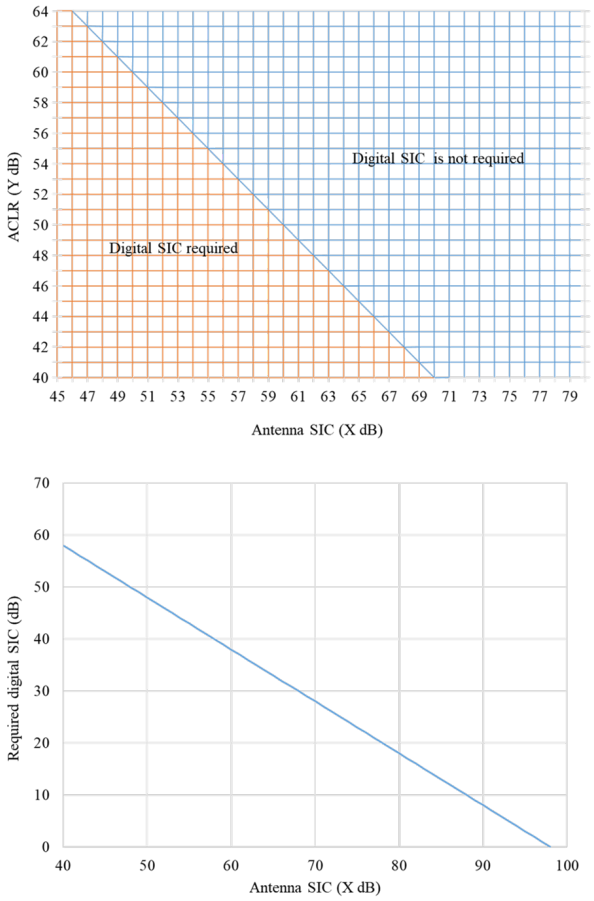

FIGURE 8. Required digital SIC in XDD systems: necessity of digital SIC with the target antenna SIC level X dB and ACLR level Y dBc (upper) and required digital SIC budget (lower).

TABLE 2. Parameters for LLS evaluation.

Parameters	Value
Carrier frequency	3.5 GHz
TX antenna height	25 m
UE antenna height	1.5 m
Target BLER	10%
Pathloss scenario	Non line-of-sight (NLOS) outdoor-to-indoor
UE speed	3 km/h
Number of UE antenna elements	2
Number or UE antenna ports	2
Number of BS antenna elements	128
Number of BS antenna ports	2
Subcarrier spacing	30 kHz
Allocated RBs	4 RBs
Occupied channel	BW 1.44 MHz
Transmission bit rate	225 kbps
Modulation and coding	QPSK/LDPC

the IR (incremental redundancy) based HARQ is applied [53]. From the results shown in Fig. 9, more than 7 dB of SNR gain is achieved for 5 times longer UL transmission with XDD.

Based on the link evaluation results, the link budget of XDD and TDD can be summarized in Table 3. The residual self-interference assumption of less than 1 dB is based on the

This article has been accepted for publication in a future issue of this journal, but has not been fully edited. Content may change prior to final publication. Citation information: DOI 10.1109/ACCESS.2021.3068977, IEEE Access

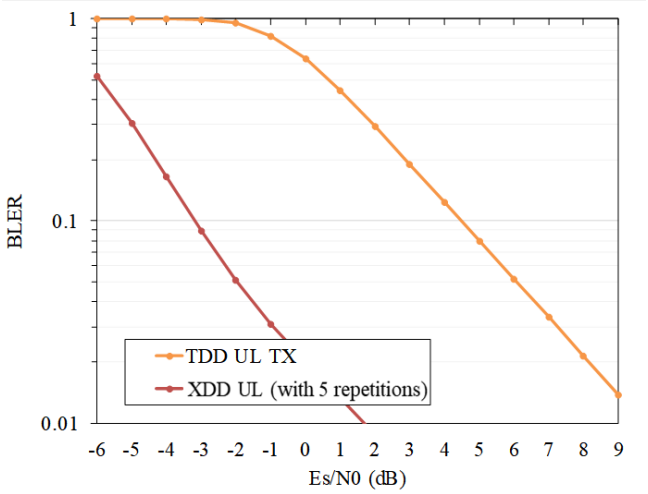

FIGURE 9. Uplink BLER performance for XDD and TDD with DL:UL=4:1 ratio where XDD makes 5 repetitive transmissions for an UL packet while TDD makes a single transmission.

TABLE 3. Uplink coverage comparison between TDD and XDD.

Quantity	TDD (DL:UL=4:1)	XDD
(a) Transmission power [dBm]	23	23
(b) TX gain [dB]	-1	-1
(c) Radiated power [dBm]	22	22
(d) Thermal noise density [dBm/Hz]	-174	-174
(e) Effective noise and interference for data channel [dB]	10	11
(f) Effective noise power [dBm]	-102.5	-102.5
(g) Required SNR from LLS [dB]	4.6	-3.0
(h) receiver sensitivity [dBm]	-96.4	-104.0
(i) RX gain and loss [dB]	26.1	26.1
(j) channel fading margin [dB]	30.7	30.7
(k) HW link budget margin [dB]	144.4	152.0
(l) Shadow fading margin [dB]	4.48	4.48
(m) Penetration margin [dB]	26.35	26.25
(n) available pathloss [dB]	107.8	114.4
Maximum radio distance [m]	136	210
Coverage area ratio	1	2.37

actual measurement taken from XDD PoC. At the UE side, the actual radiated power from the transmit antenna (c) is the sum of transmission power (a) and the effective UE TX gain (b). At the receiver (i.e., base station) side, the effective noise power (f) can be obtained as the sum of thermal noise power and the effective noise and interference power for the data channel. The thermal noise power can be calculated by the multiplication of thermal noise density (d) and the occupied channel bandwidth (e.g., 4 resource blocks in NR system). Residual interference after SIC is added in (e) for XDD. Then, two different required SINRs for TDD and XDD to satisfy the target BLER (g) for the given transmission bit rate are applied. As a consequence, the receiver sensitivity (h) can be calculated by the sum of effective noise power (f) and the required SINR (g). Taking into account the effective base station antenna gain (i) and channel fading margin (j) properly, the hardware link budget margin (k) for each duplexing scheme can be calculated ((k)=(c)+(i)-(h)). Finally, available

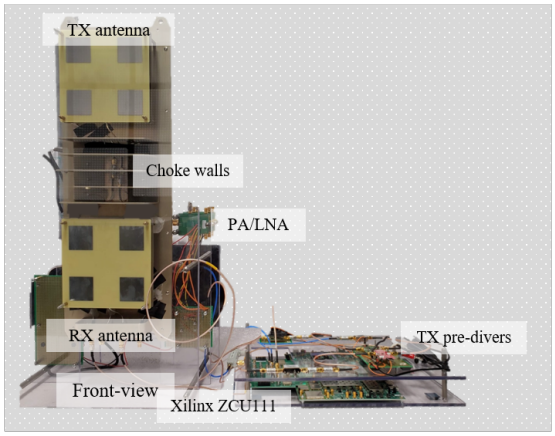

FIGURE 10. XDD PoC platform: antenna module and FPGA board.

TABLE 4. Parameters for XDD PoC.

Parameters	Value
Carrier frequency	2.4 GHz
Bandwidth	100 MHz
DL sub-band	Lower and upper 40 MHz
UL sub-band	Middle 20 MHz
DL TX power	30 dBm
UL TX power	23 dBm
XDD antenna structure	2 x 2 elements
Polarization	+45/-45 cross-polarization
TXRU structure for XDD operation	1T/1R
UL modulation	16 QAM
Pathloss	91 dB
The number of isolation wall	5
ADC/DAC resolution	12/14 bit

pathloss (n) can be calculated with shadow fading (l) and penetration margin (m), that is , (n) = (k)-(l)-(n). The analysis shows that the proposed XDD can extend the maximum UL radio distance by 54% compared with that of TDD. This radio distance improvement is equivalent to a coverage area that is 2.37 times as large as that of TDD.

A coverage area extension of 2.37 times means that the area covered by 7 conventional base stations using TDD can be operated with 3 or 4 base stations using XDD. In addition, if the coverage extension gain is transformed to the UL capacity increase, this result can be interpreted that the UL throughput can be improved by 4 times for mid-to-high SINR UEs.

V. XDD POC PROTOTYPING AND PERFORMANCE

A. XDD POC PROTOTYPE

XDD PoC system is divided into two parts (see Fig. 10). The first part is the antenna part and the other part is the FPGA part. In the case of the antenna part, there is one transmit antenna and one receive antenna, and each antenna has a 2 x 2 antenna element structure. Since the direct antennas can focus radiation energy in a certain direction toward the front, the amount of leakage signal at the UL antennas can be further reduced. In the case of the FPGA part, the SIC

algorithm is implemented in Xilinx's ZCU111 [40]. Table 4 summarizes the XDD PoC design parameters. A 40 Gbps Ethernet link is connected between a host server and the FPGA platform. This link handles 32-bit data at 122.88 MSps from one DAC and two ADCs in real-time. The DAC receives data passing through ×32 up-sampling using interpolation filters. The output of ADC is passed through decimation filters that reduce the data rate by a factor of 32. The passband channel filters are used in the TX and RX chain to reduce the images, so as to have minimized the impact on the SIC performance. To estimate and increase accuracy of SIC over the wideband siganl, e.g., 100 MHz, 491.52 Msps is used.

To estimate channel between the base station and UE, the sounding reference signal (SRS) is transmitted. To estimate leakage channel between DL to UL chain at the base station, DL reference signal is transmitted over DL only time slots before performing SIC. Detailed block diagram for XDD PoC and test setup in an anechoic chamber are depicted in Fig. 11.

To adapt parameters for DPD at the TX chain and SIC at the RX chain, at the PA output, a directional coupler is used to couple a small portion of energy through to the DPD/SIC feedback loop. A host server exchanges the IQ data samples using an Ethernet switch to place a pre-stored waveform that would play the output to the PA. The IQ data samples are computed based on the DPD polynomial and pre-distorted TX data as described in subsection III.B. The linearized PA output (after DPD) is now captured through the same path to verify performance improvement. For the UL reception of XDD operations, the RF switch is activated to provide access to the output of the LNA in the main path. The collected IQ data samples can be analyzed by a digital SIC algorithm to estimate the residual nonlinearity of the pre-distorted TX output. The residual from the digital SIC algorithm is analyzed at the host and performance metrics (e.g., EVM) computed.

B. XDD POC PERFORMANCE

The XDD PoC system is tested in an anechoic chamber with a UL signal from an emulated UE spaced 3 m away with power adjusted to simulate a cell-edge environment (see lower of Fig. 11). The DL TX power was set to 30 dBm. In the first step, both the UL and DL TXs are turned off to measure the RX noise floor. Then, the DL TX is turned on to observe the leakage power. Next, the process of DPD is executed to obtain the leakage power after DPD. Finally, the digital SIC method is conducted to obtain the residual DL cancellation power in the UL band.

The performance results are as follows in each step (see Table 5), for the performance of DPD applied in step 1, ACLR was between 40 - 45 dB if DPD is not applied, which can be improved up to 50 dB with the proposed DPD implementation. The main reason that ACLR is made as low as possible is that digital SIC can be skipped depending on antenna SIC performance. Next, in step 2, the antenna SIC performance is observed. By introducing a total of 5 walls with different heights, a distance of about twice the wavelength is required between the transmitting antenna and the receiving antenna. In the case of using the same polarization, it is possible to isolate signals of about 55 dB, and in the case of using different polarizations, 10 dB more isolation is achieved. As shown in Fig. 8, when the ACLR is 50 dB and the antenna SIC performance is 65 dB, the required digital SIC is 0 dB. In order words, using different polarizations, it can be seen that XDD can be implemented with very low complexity and without digital SIC. On the other hand, when the same polarization is used, the isolation performance is degraded by about 10 dB and a digital SIC is required for removing the whole DL leakage signal. As a result, a guard band is not required in XDD systems regardless of the digital SIC.

TABLE 5. SIC performance for XDD PoC.

SIC step	Quantity	SIC performance
Step 1	ACLR without DPD	40 - 45 dB
	ACLR with DPD	50 dB
Step 2	Isolation between port 1 (+45) to 3 (+45 degree polarization)	55 dB
	Isolation between port 1 (+45) to 4 (-45 degree polarization)	65 dB
Step 3	UL EVM in TDD mode	-24 dB
	UL EVM in XDD mode without digital SIC	-14 dB
	UL EVM in XDD mode with digital SIC	-23 dB

TABLE 6. The comparison of SIC performance.

Techniques	This work	Ref #1	Ref #2	Ref #3
Antenna SIC	65 dB	45 dB [46]	47 dB [47]	50 dB [48]
Digital SIC	30-40 dB	50 dB [49]	25 dB [50]	50 dB [51]

In order to check the performance of step 3, the worst-case using the same polarization is tested. In the case of TDD with only UL reception without DL, the received EVM of UL signal was observed to be about -24 dB. If the DL is simultaneously transmitted with UL reception without digital SIC, self-interference comes into the RX path and the EVM of UL signal is observed to be -14 dB, which degrades the performance by 10 dB. After applying the digital SIC proposed, the EVM performance is improved to a level of -23 dB, and interference is suppressed to less than 1 dB. The comparison of SIC performance is listed in Table 6 for antenna and digital SIC. For antenna SIC, various passive-based antenna cancellation or isolation techniques [46, 47, 48] shows 45 to 50 dB isolation without isolation walls while 65 dB isolation is achieved in XDD PoC. In the case of digital SIC, the SIC level of 50 dB is allowable budget for the digital SIC [49, 50, 51] with the limited ADC resolution. To handle SIC for both low and high modulation order, the budget for digital SIC should be minimized, which is 30 dB in XDD PoC.

Figures 12 and 13 show power spectral density snapshots before applying digital SIC and after digital SIC, respectively. These results are measurements of the power spectral

This article has been accepted for publication in a future issue of this journal, but has not been fully edited. Content may change prior to final publication. Citation information: DOI 10.1109/ACCESS.2021.3068977, IEEE Access

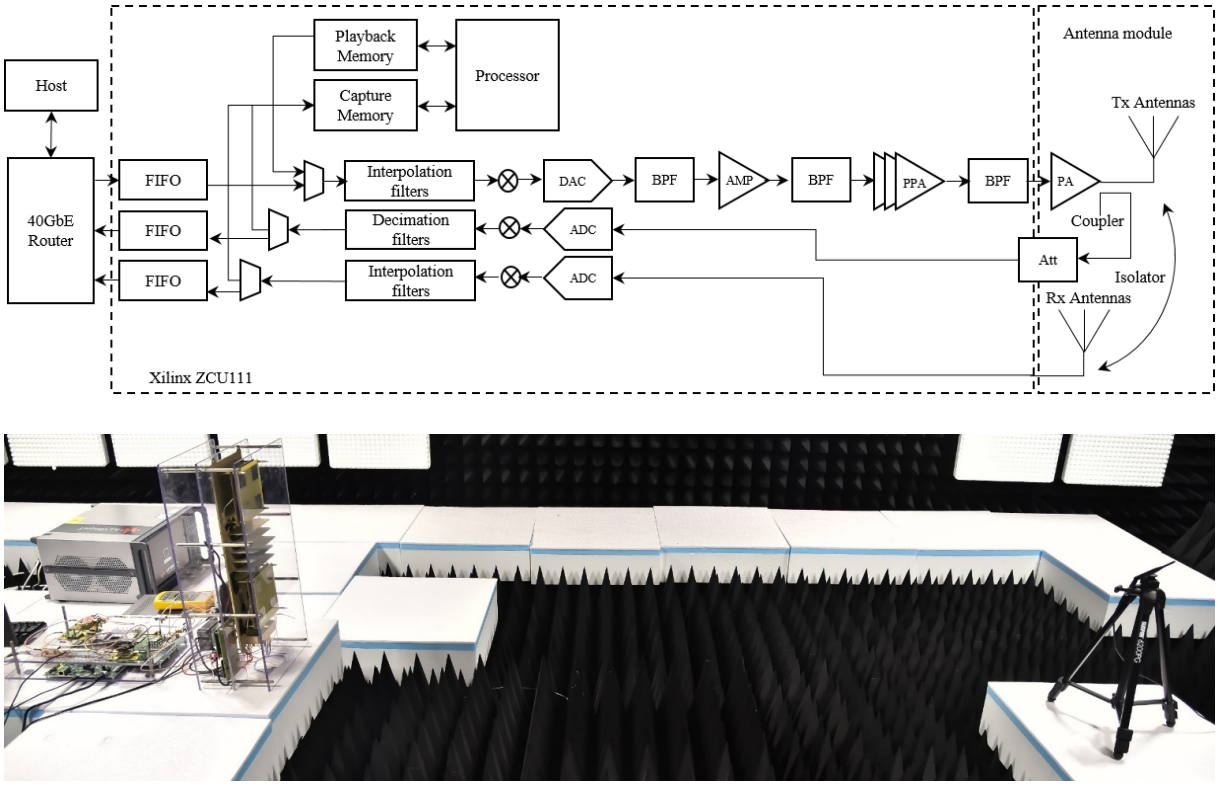

FIGURE 11. XDD PoC block diagram (upper) and test setup in an anechoic chamber (lower).

density in the frequency axis of the received UL signal observed in the RX chain. First of all, in the case of the situation without digital SIC (see Fig. 12), the interference power level of the DL is higher than the UL signal level, and it can be seen that the interference to the UL actually interferes with the ACLR of DL signal, not in-band DL signal. Since ADC saturation does not occur due to attenuation by the antenna SIC, Only 10 dB degradation is observed in the EVM of the received UL signal. After applying the digital SIC (see lower sub-figure), the interfering DL signal has completely removed from the receiver. In addition, it can be seen that the SIC performance for the UL signal is significant even when there is no guard band between the UL signals of two DL sub-bands. The reduction in guard band is possible because the entire DL interference signal is eliminated.

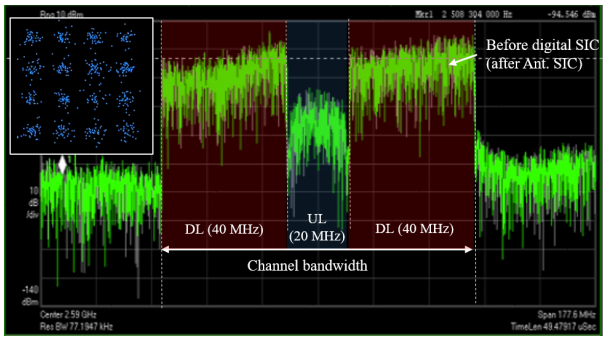

FIGURE 12. The snap shop of power spectral density and constellation of UL before applying digital SIC (with same polarization).

VI. CONCLUSION

In this paper, XDD is proposed as a means to enhance the coverage of TDD carriers. XDD enables simultaneous operations of UL and DL on the same TDD carrier but on different frequency resources. Numerical evaluations, simulations, and PoC results show that XDD can extend the UL coverage area to be more than 2 times that of TDD. It was also observed that with proper implementation of SIC, it was possible to have negligible degradation on UL reception performance even when there is almost no guard band between UL and DL signals.

While only one transmit antenna and one receive antenna are considered in this PoC, it is worth noting that XDD PoC can be implemented with relatively low complexity even when a large number of antennas are used. In general, as the number of antennas increases, the pair between the transmit and receive antennas for SIC is proportional to the square of the number of antennas. As shown in this paper, if the isolation between antennas is sufficient with DPD, in XDD, it is possible to implement the multi-antenna XDD by applying digital SIC to only a few TX/RX pairs. In future work, we will extend the XDD platform to test with actual outdoor measurements. Since the importance of TDD is increasing in order to use a wider bandwidth than FDD, the proposed XDD can be a technology that can effectively reduce the cost of installing a cellular network while securing both the

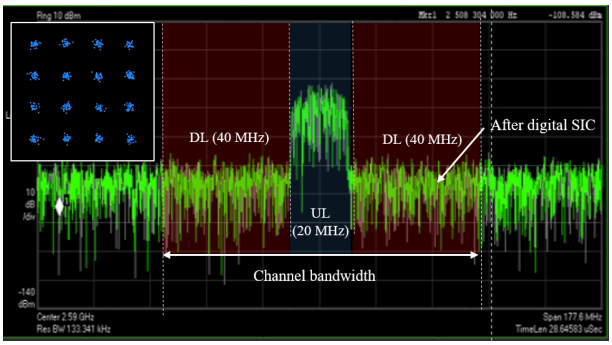

FIGURE 13. The snap shop of power spectral density and constellation of UL after applying digital SIC (with same polarization).

advantages of FDD and TDD at the same time. This advanced duplex technology will emerge as an important technology for beyond 5G and 6G in the future wireless communications.

REFERENCES

[1] J. Navarro-Ortiz, P. Romero-Diaz, S. Sendra, P. Ameigeiras, J. J. Ramos-Munoz, and J. M. Lopez-Soler, "A survey on 5G usage scenarios and traffic models," *in IEEE Commun. Surveys Tuts.*, vol. 22, no. 2, pp. 905–929, 2nd Quart., 2020.

[2] J. Yeo, T. Kim, J. Oh, S. Park, Y. Kim, and J. Lee, "Advanced data transmission framework for 5G wireless communications in the 3GPP new radio standard," *in IEEE Commun. Standards Mag.*, vol. 3, no. 3, pp. 38–43, Sep. 2019.

[3] K. Takeda, H. Xu, T. Kim, K. Schober, and X. Lin, "Understanding the heart of the 5G air interface: An overview of physical downlink control channel for 5G new radio," *in IEEE Commun. Standards Mag.*, vol. 4, no. 3, pp. 22–29, Sep. 2020.

[4] Y. Kim, F. Sun, Y.Wang, Y. Qi, J. Lee, Y. Kim, J. Oh, H. Ji, J. Yeo, S. Choi, H. Ryu, H. Noh, and T. Kim, "New radio (NR) and its evolution toward 5G-advanced," *in IEEE Wireless Commun.*, vol. 26, no. 3, pp. 2–7, Jun. 2019.

[5] Study on NR coverage enhancements (Release 17), V17.0.0, document TR 38.830, 3GPP, Dec. 2020.

[6] E. Onggosanusi et al., "Modular and high-resolution channel state information and beam management for 5G new radio," *in IEEE Commun. Mag.,* vol. 56, no 3, pp. 48–55, March 2018.

[7] User Equipment (UE) radio transmission and reception; Part 1: Range 1 Standalone (Release 16), document TS 38.101-1, 3GPP, Jun. 2020.

[8] Z. Shen, A. Khoryaev, E. Eriksson, and X. Pan,"Dynamic uplinkdownlink configuration and interference management in TD-LTE," *in IEEE Commun. Mag.*, vol. 50, no. 11, pp. 51-–59, Nov. 2012.

[9] Toni A. Levanen, Juho Pirskanen, Timo Koskela, Jukka Talvitie, Mikko Valkama, "Radio Interface Evolution Towards 5G and Enhanced Local Area Communications", *in IEEE Access,* vol. 2, pp. 1005–1029, 2014.

[10] T. L. Marzetta, "Noncooperative cellular wireless with unlimited numbers of base station antennas," *in IEEE Trans. Wireless Commun.*, vol. 9, no. 11, pp. 3590—3600, Nov. 2010.

[11] T. Kim, K. Min, M. Jung and S. Choi, "Scaling Laws of Optimal Training Lengths for TDD Massive MIMO Systems," *in IEEE Trans. Veh. Technol.*, vol. 67, no. 8, pp. 7128–7142, Aug. 2018.

[12] K. I. Pedersen, G. Berardinelli, F. Frederiksen and P. Mogensen, "A Flexible 5G Wide Area Solution for TDD with Asymmetric Link Operation," *in IEEE Wireless Commun.*, vol. 24, no. 2, pp. 122–128, April 2017.

[13] P. W. C. Chan et al., "The evolution path of 4G networks: FDD or TDD?," *in IEEE Commun. Mag.*, vol. 44, no. 12, pp. 42–50, Dec. 2006.

[14] C. She, C. Yang, and T. Q. S. Quek, "Radio resource management for ultra-reliable and low-latency communications," *IEEE Commun. Mag.*, vol. 55, no. 6, pp. 72—78, Jun. 2017.

[15] W. Kim, H. Ji and B. Shim, "Channel Aware Sparse Transmission for Ultra Low-Latency Communications in TDD Systems," *in IEEE Trans. on Commun.*, vol. 68, no. 2, pp. 1175–1186, Feb. 2020.

[16] Supplementary Uplink (SUL) and LTE-NR Co-Existence (Release 15), document TR 37.872 V15.1.0, 3GPP, Dec. 2018.

[17] Q. Feng, J. Pang, M. Maso, M. Debbah and W. Tong, "IDFT-VFDM for Supplementary Uplink and LTE-NR Co-Existence," *in IEEE Trans. on Wireless Commun.*, vol. 19, no. 5, pp. 3435–3448, May 2020.

[18] B. Yu, L. Yang, H. Ishii and S. Mukherjee, "Dynamic TDD Support in Macrocell-Assisted Small Cell Architecture," *in IEEE Journal on Selected Areas in Commun.*, vol. 33, no. 6, pp. 1201–1213, June 2015, doi: 10.1109/JSAC.2015.2417013.

[19] H. Sun, M. Sheng, M. Wildemeersch, T. Q. S. Quek and J. Li, "Traffic Adaptation and Energy Efficiency for Small Cell Networks With Dynamic TDD," *in IEEE Journal on Selected Areas in Commun.*, vol. 34, no. 12, pp. 3234–3251, Dec. 2016.

[20] T. Ding, M. Ding, G. Mao, Z. Lin, A. Y. Zomaya and D. López-Pérez, "Performance Analysis of Dense Small Cell Networks With Dynamic TDD," *in IEEE Trans. Veh. Technol.*, vol. 67, no. 10, pp. 9816–9830, Oct. 2018.

[21] D. Kim, H. Lee and D. Hong, "A Survey of In-Band Full-Duplex Transmission: From the Perspective of PHY and MAC Layers" *in IEEE Commun. Surveys & Tuts.*, vol. 17, no. 4, pp. 2017–2046, Fourthquarter 2015

[22] X. Xia, K. Xu, Y. Wang, and Y. Xu, "A 5G-enabling technology: Benefits, feasibility, and limitations of in-band full-duplex mMIMO," *IEEE Veh. Technol. Mag.*, vol. 13, no. 3, pp. 81-–90, Sep. 2018.

[23] E. Ahmed and A. M. Eltawil, "All-digital self-interference cancellation technique for full-duplex systems,"*IEEE Trans. Wireless Commun.*, vol. 14, no. 7, pp. 3519–3532, Jul. 2015.

[24] A. C. Cirik, S. Biswas, O. Taghizadeh, and T. Ratnarajah, "Robust transceiver design in full-duplex MIMO cognitive radios," *IEEE Trans. Veh. Technol.*, vol. 67, no. 2, pp. 1313-–1330, Feb. 2018.

[25] U. Singh, S. Biswas, K. Singh, B. K. Kanaujia and C. -P. Li, "Beamforming Design for In-Band Full-Duplex Multi-Cell Multi-User MIMO LSA Cellular Networks," *in IEEE Access,* vol. 8, pp. 222355–222370, 2020.

[26] E. Dahlmann, P. Beming, J. Knutsson, F. Ovesjö, M. Persson, and C. Roobol, "WCDMA—The radio interface for future mobile multimedia communuications," *IEEE Trans. Veh. Technol.*, vol. 47, pp. 1105-–1118, Nov. 1998.

[27] E. Dahlmann, B. Gudmundson, M. Nilsson, and J. Sköld, "UMTS/IMT-2000 based on wideband CDMA," IEEE Commun. Mag., Sept. 1998.

[28] M. Haardt et al., "The TD-CDMA based UTRA TDD mode,"*in IEEE Journal on Selected Areas in Commun.*, vol. 18, no. 8, pp. 1375-1385, Aug. 2000.

[29] S. Yun et al., "Hybrid Division Duplex System for Next-Generation Cellular Services," *in IEEE Trans. Veh. Technol.*, vol. 56, no. 5, pp. 3040–3059, Sept. 2007, doi: 10.1109/TVT.2007.900389.

[30] M. Afshang, Z. Yazdanshenasan, S. Mukherjee, P. Chong, "Hybrid division duplex for HetNets: Coordinated interference management with uplink power contro," *on Communication Workshop (ICCW) 2015 IEEE International Conference*, pp. 106–112, 2015.

[31] Y. S. Soh, T. Q. S. Quek, M. Kountouris and G. Caire, "Cognitive Hybrid Division Duplex for Two-Tier Femtocell Networks," *n IEEE Trans. on Wireless Commun.*, vol. 12, no. 10, pp. 4852–4865, October 2013.

[32] T. M. Kim, H. J. Yang, and A. J. Paulraj, "Distributed sum-rate optimization for full-duplex MIMO system under limited dynamic range," *IEEE Signal Process. Lett.*, vol. 20, no. 6, pp. 555—558, Jun. 2013.

[33] Y. Liu, C. Huang, X. Quan, P. Roblin, W. Pan and Y. Tang, "Novel Linearization Architecture with Limited ADC Dynamic Range for Green Power Amplifiers," *in IEEE Journal on Selected Areas in Commun.*, vol. 34, no. 12, pp. 3902–3914, Dec. 2016.

[34] T. Ranström and E. Axell, "Full Duplex Based Digital Out-of-Band Interference Cancellation for Collocated Radios," *IEEE Wireless Commun. and Networking Conference (WCNC)*, Seoul, Korea (South), 2020.

[35] D. Korpi, T. Riihonen, V. Syrjälä, L. Anttila, M. Valkama and R. Wichman, "Full-Duplex Transceiver System Calculations: Analysis of ADC and Linearity Challenges," *in IEEE Trans. on Wireless Commun.*, vol. 13, no. 7, pp. 3821–3836, July 2014.

[36] A. Kiayani, L. Anttila, and M. Valkama, "Modeling and dynamic cancellation of TX-RX leakage in FDD transceivers," *in 2013 IEEE 56th International Midwest Symposium on Circuits and Systems (MWSCAS),* , Aug. 2013.

[37] J. Wood, "System-Level Design Considerations for Digital Pre-Distortion of Wireless Base Station Transmitters," it in IEEE Trans. on Microwave Theory and Techniques, vol. 65, no. 5, pp. 1880–1890, May 2017.

[38] D. R. Morgan, Z. Ma, J. Kim, M. G. Zierdt and J. Pastalan, "A Generalized Memory Polynomial Model for Digital Predistortion of RF Power Amplifiers," *in IEEE Trans. on Signal Processing*, vol. 54, no. 10, pp. 3852–3860, Oct. 2006.

[39] A. Tikhonov, and et al. Nonlinear ill-posed problems. London: Chapman & Hall, ISBN 0412786605, Aug 2018.
[40] Zynq UltraScale+ RFSoC ZCU111 [Online] Available: https://www.xilinx.com/products/boards-and-kits/zcu111.html
[41] I. V. Lindell and A. H. Sihvola, "Realization of the PEMC boundary," *in IEEE Trans. on Antennas and Propagation*, vol. 53, no. 9, pp. 3012–3018, Sept. 2005, doi: 10.1109/TAP.2005.854524.
[42] M. A. Hussein, V. A. Bohara, and O. Venard, "On the system level convergence of ILA and DLA for digital predistortion," *in Proc. Int. Symp. Wireless Commun. Syst. (ISWCS)*, Aug. 2012, pp. 870–874.
[43] H. Alves, T. Riihonen and H. A. Suraweera, Full-Duplex Communications for Future Wireless Networks. Springer, 2020.
[44] S. Sadjina, C. Motz, T. Paireder, M. Huemer and H. Pretl, "A Survey of Self-Interference in LTE-Advanced and 5G New Radio Wireless Transceivers," in IEEE Transactions on Microwave Theory and Techniques, vol. 68, no. 3, pp. 1118-1131, March 2020, doi: 10.1109/TMTT.2019.2951166.
[45] C. Motz, T. Paireder, H. Pretl and M. Huemer, "A Survey on Self-Interference Cancellation in Mobile LTE-A/5G FDD Transceivers," in IEEE Transactions on Circuits and Systems II: Express Briefs, doi: 10.1109/TCSII.2021.3051101.
[46] E. Everett, A. Sahai and A. Sabharwal, "Passive Self-Interference Suppression for Full-Duplex Infrastructure Nodes," in IEEE Transactions on Wireless Communications, vol. 13, no. 2, pp. 680-694, February 2014, doi: 10.1109/TWC.2013.010214.130226.
[47] E. Ahmed, A. M. Eltawil and A. Sabharwal, "Rate Gain Region and Design Tradeoffs for Full-Duplex Wireless Communications," in IEEE Transactions on Wireless Communications, vol. 12, no. 7, pp. 3556-3565, July 2013, doi: 10.1109/TWC.2013.060413.121871.
[48] S. Li and R. D. Murch, "An Investigation Into Baseband Techniques for Single-Channel Full-Duplex Wireless Communication Systems,.. in IEEE Transactions on Wireless Communications, vol. 13, no. 9, pp. 4794-4806, Sept. 2014, doi: 10.1109/TWC.2014.2341569.
[49] C. D. Nwankwo, L. Zhang, A. Quddus, M. A. Imran and R. Tafazolli, "A Survey of Self-Interference Management Techniques for Single Frequency Full Duplex Systems," in IEEE Access, vol. 6, pp. 30242-30268, 2018, doi: 10.1109/ACCESS.2017.2774143.
[50] D. Korpi, Y. Choi, T. Huusari, L. Anttila, S. Talwar and M. Valkama, "Adaptive Nonlinear Digital Self-Interference Cancellation for Mobile Inband Full-Duplex Radio: Algorithms and RF Measurements," 2015 IEEE Global Communications Conference (GLOBECOM), San Diego, CA, USA, 2015, pp. 1-7, doi: 10.1109/GLOCOM.2015.7417188.
[51] J. W. Kwak, M. Soo Sim, I. Kang, J. S. Park, J. Park and C. Chae, "A Comparative Study of Analog/Digital Self-Interference Cancellation for Full Duplex Radios," 2019 53rd Asilomar Conference on Signals, Systems, and Computers, Pacific Grove, CA, USA, 2019, pp. 1114-1119, doi: 10.1109/IEEECONF44664.2019.9048978.
[52] E. G. Larsson, O. Edfors, F. Tufvesson and T. L. Marzetta, "Massive MIMO for next generation wireless systems," in IEEE Communications Magazine, vol. 52, no. 2, pp. 186-195, February 2014, doi: 10.1109/MCOM.2014.6736761.
[53] J. H. Bae, A. Abotabl, H.-P. Lin, K.-B. Song, and J. Lee, "An overview of channel coding for 5G NR cellular communications," APSIPA Transactions on Signal and Information Processing, vol. 8, p. e17, 2019.

HYOUNJU JI (M'13–SM'20) received the B.S. and M.S. degrees in electronic engineering from Sogang University, and the Ph.D. degree in electrical engineering from Seoul National University. He joined Samsung Electronics in 2007, where he has been involved in 3GPP RAN1 LTE, LTE-Advanced, LTE-Advanced Pro, and 5G NR technology developments and standardizations. He is currently a Principal Engineer with Samsung Electronics. His current research interests include advanced duplex scheme, multi-antenna techniques, compressed sensing, massive connectivity, machine type communications, URLLC, and IoT communications.

YOUNSUN KIM (SM'20) received the B.S. and M.S. degrees in electronic engineering from Yonsei University, in 1996 and 1999, respectively, and the Ph.D. degree in electrical engineering from the University of Washington, in 2009. He joined Samsung Electronics in 1999, and has since worked on the physical layer standardization of cdma2000, HRPD, LTE, and NR. He has been serving as the Vice-Chairman of the 3GPP RAN1 (physical layer) working group since 2017. He is currently a Master (Technical VP) with Samsung Electronics and leads the research on physical layer standardization of wireless communications.

KHURRAM MUHAMMAD (M'93–SM'09) received a Ph.D. degree from Purdue University, West Lafayette, IN in 1999 in electrical engineering. He has worked as a technology development leader in several companies for over 20 years including Samsung Electronics, Phazr, MediaTek, Mstar Semiconductor, Blackberry and Texas Instruments. He is a Director at Samsung Research America in Plano, TX leading an RF Systems Team addressing 6G communication and PoC systems. He holds 90 patents and has published more than 80 papers in IEEE journals and conferences in the areas of VLSI, cellular and connectivity communications. He is an expert on System-on-chip design from baseband to RF frontends addressing communications and radar signal processing.

CHANCE TARVER received the B.S. degree in electrical engineering from Louisiana Tech University, Ruston, LA, USA, in 2014, and the M.S. degree in electrical and computer engineering from Rice University, Houston, TX, USA, in 2016, where he is currently pursuing the Ph.D. degree with the Department of Electrical and Computer Engineering. His current research interests include physical layer impairments and signal processing for massive MIMO.

MATTHEW TONNEMACHER received the B.S., M.S., and Ph.D. degrees in electrical engineering from Southern Methodist University, Dallas, Texas, in 2011, 2013, and 2019, respectively. He has been with Samsung Research America in Plano, Texas since 2016 as a wireless systems engineer. His current research interests include spectrum sharing, software defined radio, and next generation wireless technologies.

TAEHYOUNG KIM received the B.S. and Ph.D. degrees in electrical and electronic engineering from Yonsei University, Seoul, South Korea, in 2010 and 2016, respectively. He joined Samsung Electronics in 2016, and has been working on the standardization of 5G wireless communication systems in 3GPP. His research interests include signal processing for communications, massive MIMO systems, and frame structure design.

JINYOUNG OH received Ph. D degree in wireless communication from Korea Advanced Institute of Science and Technology (KAIST) in 2013. He joined Samsung Electronics in 2013 and has been working on standardization of LTE and 5G air-interface research and system design.

BIN YU received his M.S. in Electrical engineering from university of Southampton, United Kingdom. He is currently a director of communication research lab in Beijing Samsung Telecom R&D Center of Samsung Electronics, leading 5G & Beyond adv. research for physical layer. He has 10+ years' experience in mobile communication field and has been working on various standards, incl. TD-SCDMA, HSPA+, LTE and LTE-A since from July 2006. His current research interests include advanced waveform, non-orthogonal multiple access, flexible duplexing, artificial intelligent assisted wireless etc.

GARY XU (M'99) received his B.S. in Electrical Engineering from Tsinghua University, Beijing, China and M.S. in Electrical and Computer Engineering from Rice University, Houston, TX in 1996 and 1999, respectively. He is currently a Sr. Director of Research at Standards and Mobility Innovation Lab, Samsung Research America, where he leads an RF systems and circuits team on the prototyping of beyond 5G and 6G cellular systems. He led the world's first Full Dimension MIMO (FD-MIMO/massive MIMO) prototype development and successfully demonstrated commercial feasibility in 2015. Before joining Samsung, he was with Texas Instruments from 2006 to 2012 working on RF and modem system design for cellular and IoT products, and with Nokia Research Center from 1999 to 2006, where he led the 3GPP HSPA prototype development.

JUHO LEE (F'19) received the Ph.D. degree in electrical engineering from the Korea Advanced Institute of Science and Technology (KAIST), South Korea, in 2000. He is currently a Fellow (Technical SVP) with Samsung Electronics, where he is leading research and standardization for mobile communications. He joined Samsung Electronics, in 2000, and has worked on 3G, 4G, and 5G technologies and is leading research for future technologies, such as beyond 5G and 6G. He was a Vice Chairman of 3GPP RAN WG1 from February 2003 to August 2009 and chaired LTE/LTE-Advanced MIMO sessions.